D3.5 Report on high-accuracy indoor localization under privacy constraints

Quanfeng Wang, Alexander Paulus, Matthias Saurer, Thomas Eibert

Grant Agreement Number	101099491
Action Acronym	HOLDEN
Action Title	Ethical Design of Holography with Dense wireless Networks (HOLDEN)
Funding Scheme	HORIZON-EIC-2022-PATHFINDEROPEN-01
Version date of the Annex I against which the assessment will be made	13/12/2022
Start date of the project	1/6/2023
Due date of the deliverable	30/11/2024
Actual date of submission	29/11/2024
Responsible	TUM
Contributors	TUM
Dissemination level	Public

European Innovation Council

Funded by the European Union

Funded by the European Union. Views and opinions expressed are, however, those of the author(s) only and do not necessarily reflect those of the European Union or European Innovation Council and SMEs Executive Agency (EISMEA). Neither the European Union nor the granting authority can be held responsible for them. Grant Agreement No: 101099491.

Authors in alphabetical order

Full Name	Organisation	E-mail
Quanfeng Wang	TUM	quanfeng.wang@tum.de
Alexander Paulus	TUM	a.paulus@tum.de
Matthias Saurer	TUM	matthias.saurer@tum.de
Thomas Eibert	TUM	eibert@tum.de

Change History

Version	Date	Status	Author (Company)	Description
1.0	12.11.2024	Final	TUM	First final version

Executive Summary

Outdoor positioning techniques and their applications have become relatively mature over the past years, while indoor positioning technologies have emerged as a popular research area with the widespread adoption of wireless electronic devices. In the foreseeable future, there will be a growing demand for higher standards in accuracy, ease of implementation, and cost-effectiveness in indoor localization techniques. At the same time, accompanying challenges, such as privacy concerns, will also become more pressing. The collection and use of sensitive data raise privacy concerns that must be effectively managed to protect user information and comply with legal regulations.

In this deliverable, based on the concerns (and potential opportunities) that have been collected and expressed by all project partners in the ethics status monitor (ESM) [1], we present a privacy-compliant passive tag design for indoor localization. By utilizing the advanced imaging technique introduced in D3.2, simple and low-cost passive tags can be efficiently implemented for localization and personal identification. Unlike traditional indoor positioning technologies, the positioning technique discussed in this deliverable operates at the imaging level, where passive tags function merely as simple scatterers. Using powerful holographic passive imaging techniques, the location of the tags can be accurately reconstructed. Imaging techniques, leveraging the characteristics of passive radar, utilize measurements of electromagnetic waves present in the environment without the need for additional hardware or extra spectrum bandwidth. Moreover, different shapes of the tags allow for the intuitive distinction of individuals or objects. Additionally, the application of this positioning technique can be largely customized by the user, making it adaptable to privacy and ethical considerations.

The following contents are covered:

- Short introduction of the HOLDEN project and the collaboration partners
- Reviewing of the indoor localization techniques
- Passive tags for indoor localization utilizing inverse source based imaging technique
- Privacy and ethical considerations of the passive tag design
- Numerical simulations and experimental measurements results

Table of Contents

Abbreviations

Abbreviation	Description
3D	three-dimensional
Aalto	Aalto University
CNR	Consiglio Nazionale Ricerche
CSI	channel state information
EC	European Commission
EM	electromagnetic
ESM	Ethics Status Monitor
EU	European Union
HE	Horizon Europe
HOLDEN	Ethical design of holography in dense wireless networks
IoT	Internet of Things
MTC	Machine Type Communication
PEC	perfect electric conductor
RF	radio frequency
RFID	radio frequency identification device
RSSI	received signal strength indicator
TDoA	time difference of arrival
ToF	time of flight
TOI	target of interest
TUM	Technical University of Munich
TWE	University of Twente

WP	work package

1. Introduction

1.1. About HOLDEN

The ubiquitous perception by sensing of objects, subjects and gestures is a pivotal challenge for future technology: it enables personalized services such as smart living, automated logistics or interaction through free-space gestures. However, it also challenges ethical and moral boundaries and threatens privacy. HOLDEN proposes a radically new approach to perception by concisely analysing ethical constraints and privacy risks while re-thinking RF-based sensing. We establish necessary conditions for privacy preserving and ethically compliant sensing and develop new paradigms respecting these constraints.

For the first time ever, HOLDEN constitutes a concentrated effort to explore social aspects of RF-sensing to guide the technological advance and to derive technology for ethically and privacy compliant perception. Central to HOLDEN is the development of ethical and privacy constraints. We use these findings to derive privacy and ethically compliant concepts for RF-based perception. We will develop a system of distributed multi-antenna devices for simultaneous multitarget recognition and ubiquitous perception with unprecedented accuracy, which constitutes a radical paradigm shift from a technology-centric perspective to a privacy-centric one via privacy by design.

HOLDEN achieves this goal along three high risk, complementary, and privacy-centric paths:

Path 1: Continuous-space measurement points: Radio-based 3D vision by holographic image processing of RF wavefronts.

Path 2: Discrete-space measurement points: Advanced 3D beamforming for human-scale recognition and tracking through dense massive connected antenna arrays.

Path 3: Signal processing and learning: High-dimensional tensor processing for the distinction of complex activities and motion from massive-dimensional RF data. The resulting breakthrough approaches and algorithms will be compared against application-level benchmarks via usage scenarios in the fields of logistics, smart living, and free-space

1.2. Partners

The consortium consists of four academic partners and a high-tech SME partner: (a) Aalto University (AALTO), Finland, (b) Technical University of Munich (TUM), Germany, (c) Consiglio Nazionale Ricerche (CNR), Italy, (d) University of Twente (TWE), Netherlands, and (e) Adant (Adant), Italy. This consortium features the specialized and complementary expertise required to achieve the project objectives. AALTO will be responsible for the project management (WP1), covered by an experienced and dedicated project manager. Ethical aspects (WP2), will be addressed by TWE (Prof. Ciano Aydin) who is a pioneer in the field. In particular, eventual gender differences in the ethical perception will be taken into account. TUM pioneered RF holography, which makes TUM (Prof. Thomas Eibert) the ideal leader of WP3. In advanced distributed signal and information processing, CNR has through Prof. Stefano Savazzi and Vittorio Rampa more than 14 years of

experience. CNR will lead WP4. Since more than 10 years, AALTO is active in radio sensing and machine learning based activity recognition. This expertise makes AALTO (Prof. Sigg) the ideal leader of WP5. Adant (Daniele Piazza) will contribute to the market analysis, application possibilities, and validation (WP6). Led by AALTO, dissemination with the website as one the media will be addressed by all partners. All academic partners are committed to early publication of results, e.g., via arXiv (open science).

2. Review of Indoor Localization

Indoor localization deals with the estimation of the position of living entities or objects within closed environments and has been extensively investigated in the past few decades. Being able to determine the location of humans or objects for example is critical for applications in sectors such as healthcare [1], disaster management [3], smart buildings [4], Internet of Things (IoT) [5], and Machine Type Communication (MTC) [6], where precise location data enables enhanced services, security, and operational efficiency.

Broadly speaking, the field of indoor positioning can be divided into two categories, active localization and passive localization. A widely accepted classification criterion in this field is that active localization determines the location of specific targets by positioning devices or tags carried by the targets, whereas passive localization does not rely on any devices or tags, nor does it require any participation from the target during the localization process [7]. Based on this classification, the localization technology discussed in this deliverable technically falls under active localization. However, the passive tags we discuss differ from most techniques in this field, where this distinction will be discussed in detail later.

In previous research on indoor localization technologies, various methods have been proposed. With the advancement of wireless communication technologies and the widespread use of portable electronic devices, radio frequency (RF)-based indoor positioning has gained considerable attention [8]. Examples include indoor localization systems based on wireless communication technologies such as WiFi [9]-[13], Bluetooth [14]-[16] and ZigBee [17].

At the same time, diverse localization algorithms, which utilize information such as received signal strength indicator (RSSI) [9], channel state information (CSI) [12], time of flight (ToF) [18], and time difference of arrival (TDoA) [19], have been successfully applied in this field. Particularly in RF-based indoor localization, radio frequency identification device (RFID) technology is widely used [20]-[24], which is based on the transmission of data through communication between RFID tags and corresponding RFID readers. RFID tags are categorized into active RFID and passive RFID, with the key difference being whether the tag has an independent power source [8]. Active RFID tags are connected to a specific power supply, enabling communication over several hundred meters with low-cost circuit design, but with limited positioning accuracy [8]. On the other hand, passive RFID tags operate without batteries, as they extract the required energy from the illuminating electromagnetic wave. However, their communication range is typically limited to just 1 or 2 meters [8], significantly constraining their application in indoor positioning.

One of the major distinctions between the passive tags discussed in this deliverable and RFID tags is that the proposed passive tags do not rely on the response or transmission of certain types of signals. Instead, the localization only relies on the electromagnetic scattering characteristics of the tags. From this perspective, the "passive" nature of the proposed tags is fundamentally different from that of RFID techniques, which might modulate the scattered signal and, thus, communicate with the reader.

In addition, other common indoor localization modalities include technologies such as visible light [25],[26], acoustic signals [27] [28], ultrasound [29] [30], magnetic fields [31] [32] and physical excitation such as floor pressure [33] and structural vibrations [1]. However, these approaches fall outside the scope of this deliverable and will not be discussed in detail. Vision-based indoor localization systems, for example known as camera-based or image-based localization techniques, should be mentioned. This type of technology is widely used in fields such as surveillance [34] and crowd counting [35]. It typically relies on specific imaging systems, e.g., Kinect cameras are used under good visible light conditions [36], while infrared cameras are employed for thermal imaging in low-visibility environments [37]. Under this premise, previous research has primarily focused on extracting precise location information from the obtained RGB or thermal images. Many related techniques, such as colour histograms [39], automatic indexing methods [40], and transfer learning [41], have been proposed.

However, one of the most criticized aspects of these vision-based methods is the use of cameras, which raises significant concerns regarding user privacy [38]. In addition to the fact that location information is inherently sensitive for users—many of whom may be unwilling to share such data—the use of optical or infrared cameras for indoor scene imaging can cause significant discomfort. In fact, most existing indoor localization systems have not adequately addressed privacy and ethical concerns [8]. Most of them focus solely on positioning accuracy. This undoubtedly hampers the development and commercialization of positioning technologies.

The indoor localization method and passive tags studied in this deliverable are based on the microwave imaging algorithms discussed in D3.2 and can be viewed as a hybrid of RF-based and vision-based indoor localization. A detailed discussion of the privacy and ethical aspects of the imaging algorithm has already been provided in D3.2 and will not be repeated here. The technical details of the localization and identification method based on this privacy-conscious holographic imaging algorithm, along with related privacy considerations, will be thoroughly presented in this deliverable.

3. Passive Tags Based on Holographic Imaging

3.1. Imaging Behaviour of Passive Tags

The indoor localization technique discussed in this deliverable is based on the powerful 3D holographic imaging algorithm proposed in D3.2. Under the illumination of a specific source, the scattered electromagnetic field from a scattering object is captured by a moving measurement probe or probe array, which can then be post-processed for imaging purposes. Utilizing this imaging algorithm, the spatial position of the electromagnetic scatterers, including the passive tags, can be easily obtained. The details of the imaging algorithm have been provided in D3.2.

One requirement for the passive tags in this process is that they must scatter a measurable electromagnetic field when illuminated, meaning that theoretically any sufficiently strong electromagnetic scatterer can serve as a passive tag. Other important properties of passive tags are their shape, which could potentially be used to distinguish between different individuals.

The first example we consider for the realisation of a simple passive tag is a patch antenna, as shown in Fig. 1.

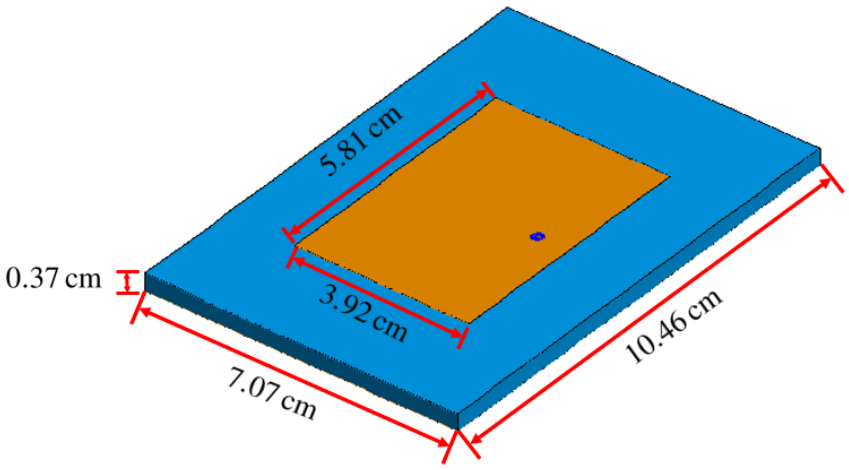

Fig. 1. Example of a patch antenna as passive tag.

The substrate dimensions of the patch antenna are $10.46\,\mathrm{cm} \times 7.07\,\mathrm{cm}$, with a thickness of $0.37\,\mathrm{cm}$ and a relative permittivity of 2.15. The thin patch is made of perfectly electrically conducting (PEC) material, with dimensions of 5.81 cm × 3.92 cm. The feed point is located at the center of the long edge of the patch, offset by 1.24 cm from the center along the short edge. The antenna is designed to resonate at a frequency of 2.4 GHz, ensuring that it generates the largest possible scattered electromagnetic field within the simulation frequency range for imaging.

The patch antenna, serving as a passive tag, is positioned on the chest of a human model at a height of approximately 1.25 meters, as shown in Fig. 2. The height of the human body is around

1.8 meters. The body material is assumed to consist primarily of muscle, and the corresponding parameters, such as the relative permittivity and dielectric loss tangent, are retrieved from an online simulator [42].

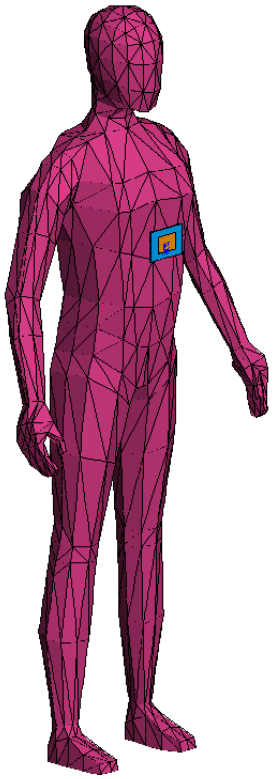

Fig. 2. Illustration of the simulation setup in FEKO including a human model and a patch antenna serving as the passive tag.

Simulations were carried out using the commercial full-wave simulation software FEKO [43]. The human body and the passive tag are placed around the origin of the coordinate system. The illuminating source is a Hertzian dipole located at the coordinates $x = 0\ \mathrm{m}$, $y = 2\ \mathrm{m}$, $z = 1\ \mathrm{m}$. which is roughly 2 meters in front of the body model, at a height close to the abdomen. This setup aims to illuminate the whole body equally. The x- and z-components of the electric field were collected over a rectangular aperture in the plane $y = 0.5\ \mathrm{m}$ extending from $x = -3\ \mathrm{m}$, $z = -3\ \mathrm{m}$ to $x = 3\ \mathrm{m}$, $z = 3\ \mathrm{m}$, positioned directly in front of the human body to capture more scattered fields. Overall, $12\,100$ uniformly distributed probe positions on the measurement plane are sampled to fulfil the minimum sampling requirement and ensure a proper resolution of the image. In practice, this measurement can be done by a single moving probe antenna or, more desirable, an electronically switched antenna array.

The utilized frequencies are linearly distributed from 2 GHz to 4 GHz with a step size of 50 MHz. By performing the imaging algorithm in D3.2, the final imaging results presented in Fig. 3 are obtained. The reconstruction area is constrained in a cubic space with the boundaries $-0.5\ \mathrm{m} \leqslant x \leqslant 0.5\ \mathrm{m}$, $-0.2\ \mathrm{m} \leqslant y \leqslant 0.2\ \mathrm{m}$ and $-0.1\ \mathrm{m} \leqslant z \leqslant 1.9\ \mathrm{m}$. The normalized current densities are

mapped onto the faces of the cuboid enclosing the imaging region via a maximum intensity projection, where the front view and the side view are shown in Fig. 3(a) and Fig. 3 (b), respectively. For comparison, another simulated imaging result, which includes only the human body without the passive tag, is provided in Fig. 4. From these two results, the bright spot on the chest of the human body is clearly visible, indicating the location of the passive tag.

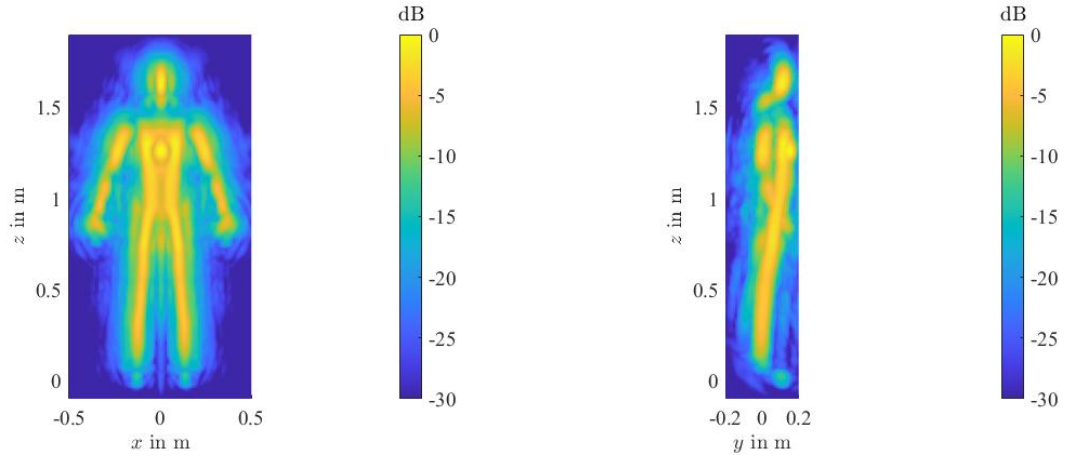

(a) (b)

Fig. 3. Multi-frequency imaging results of the human body with a passive tag obtained by the imaging algorithm in D3.2. (a) Maximum intensity projection of front view. (b) Maximum intensity projection of side view.

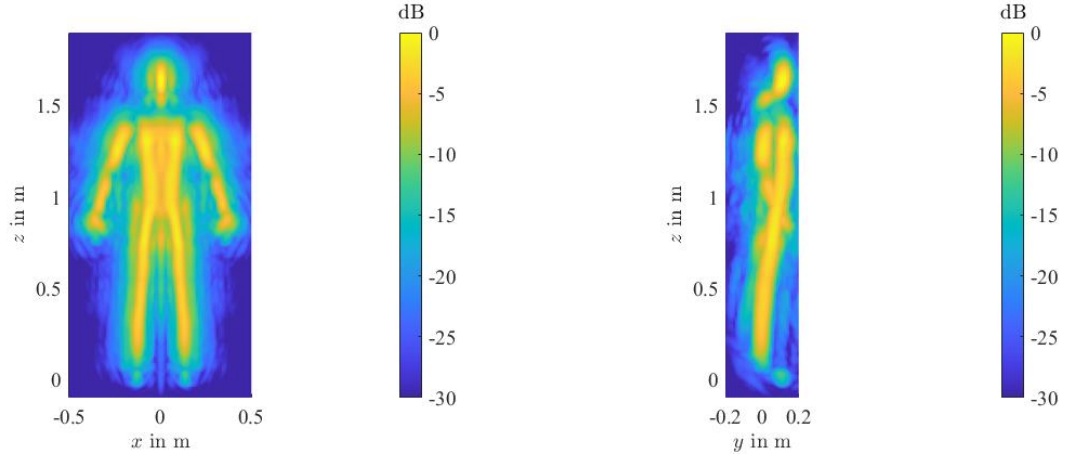

(a) (b)

Fig. 4. Imaging results of the human body without the passive tag. (a) Maximum intensity projection of front view. (b) Maximum intensity projection of side view.

For a more intuitive display, the imaging results are visualized in the form of a 3D point cloud as displayed in Fig. 5. For display purposes, the dynamic range has been adjusted to span from -10 dB

to 15 dB to ensure that the actual induced sources over the surface of the human body are not obscured by surrounding clutter.

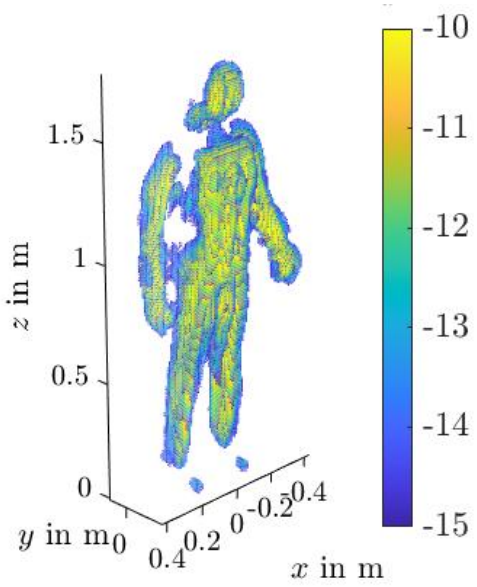

Fig. 5. 3D visualization of the imaged human body with a passive tag.

In these imaging results, the spatial relationship between the object being imaged and the measurement plane remains invariant. Therefore, as long as the exact position of the measurement plane in space is known, the location of the passive tag can be easily determined from the imaging results such as shown in Fig. 4. However, it is important to note that the resolution of the imaging system limits the accuracy of the localization. In Fig. 5, the passive tag is almost merged with the human body due to the limited range resolution. The theoretical limits for the resolution in planar measurements can be estimated as

$$\delta_x = \frac{\lambda_c y_0}{L_x}, \quad \delta_z = \frac{\lambda_c y_0}{L_z}, \quad \text{and} \quad \delta_y = \frac{c_0}{B}, \tag{3.1}$$

where L_x and L_y denote the aperture size and B is the bandwidth. λ_c represents the wavelength at the center-frequency and c_0 is the speed of light. uis the range distance between the image plane and the observation aperture. This is the best resolution that we can expect and it is limited at the physical level, which cannot be surpassed by imaging technologies without prior knowledge. Therefore, this is also the limitation of the localization method. This explains why the passive tag appears almost indistinguishable from the human body in the range direction. The frequency range considered provides a resolution of approximately 15 cm, while the closest distance between the passive tag and the surface of the human body is only 3 cm.

3.2. Identification by Passive Tags

Since the indoor localization method is based on the characteristics of the imaging algorithm, and as previously mentioned, in principle any sufficiently strong electromagnetic scatterer can serve as

a passive tag for imaging, the localization system discussed in this deliverable can also enable identification of people or objects. This is typically challenging in conventional microwave imaging. The resolution limitations and the absence of visually recognizable colour information, unlike optical imaging, pose constraints on distinguishing between individuals or objects.

However, in the scenario we consider, this issue can be addressed by designing passive tags with different shapes. When the resolution is sufficient, these uniquely shaped passive tags enable reliable identification of people or objects.

To demonstrate this, several simple PEC scatterers with different shapes were used as passive tags replacing the previously discussed patch antenna. These new passive tags were simulated alongside the human model using again FEKO. As shown in Fig. 6, a cross-shaped structure was positioned directly below the right hand of the human model. With all other simulation settings remained unchanged, the imaging result is presented in Fig. 7.

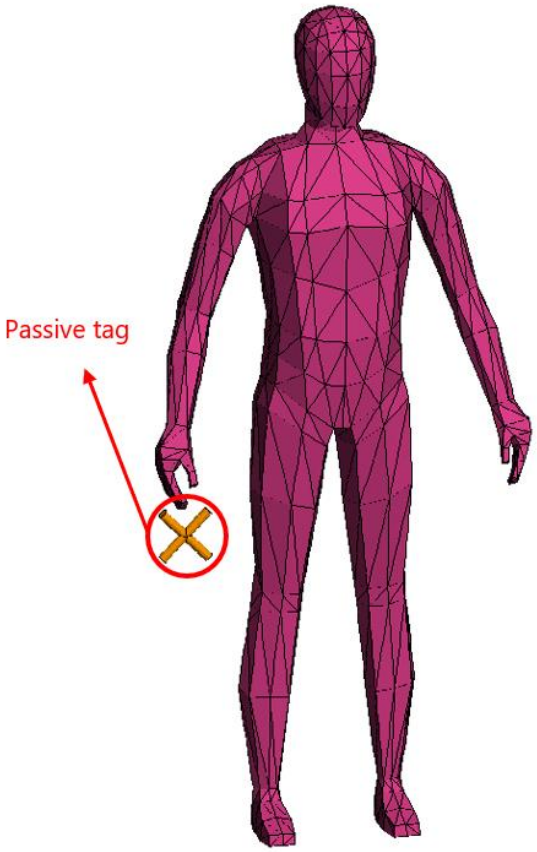

Fig. 6. Illustration of the simulation setup in FEKO including a human model and a cross-shaped PEC scatterer serving as the passive tag.

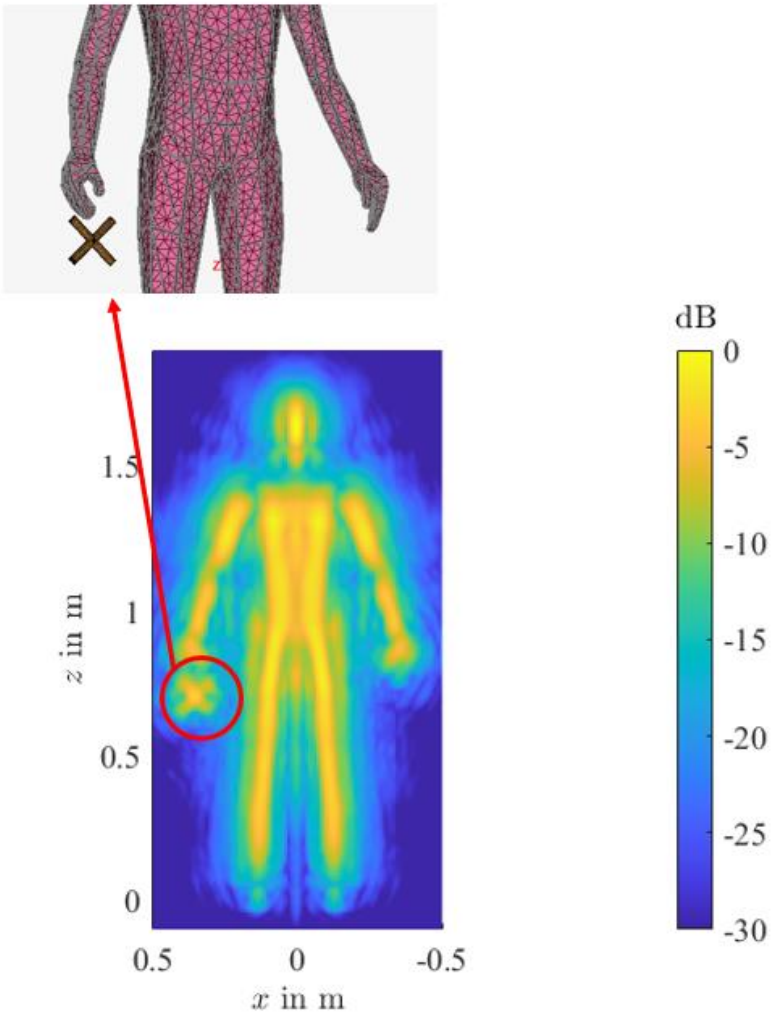

Fig. 7. Imaging result of the human body with the cross-shaped passive tag, where the zoomed-in view of the passive tag is provided.

The results shown in Fig. 7 allow to clearly distinguish between the human model and the cross-shaped structure located beneath the model's hand. This characteristic can serve as an identifier for individuals. By having different people wear distinct types of tags, it becomes possible to identify different individuals, especially those with similar body shapes. Similarly, the 3D point cloud imaging results are provided in Fig. 8.

Two additional similar simulations and imaging results are presented in Fig. 9, where Fig. 9(a) shows a square-shaped passive tag, and Fig. 9(b) shows a triangular-shaped passive tag. In Fig. 10(a), the simulation was conducted with a dog model and the cross-shaped passive tag. Maintaining the same material parameters for modelling muscle tissues, the imaging result is shown in Fig. 10(b). These results further validate the proposed positioning and identification method.

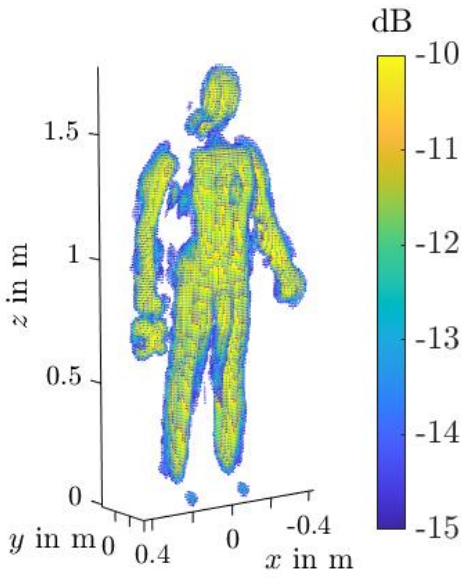

Fig. 8. 3D visualization of the imaged human body with the cross-shape passive tag.

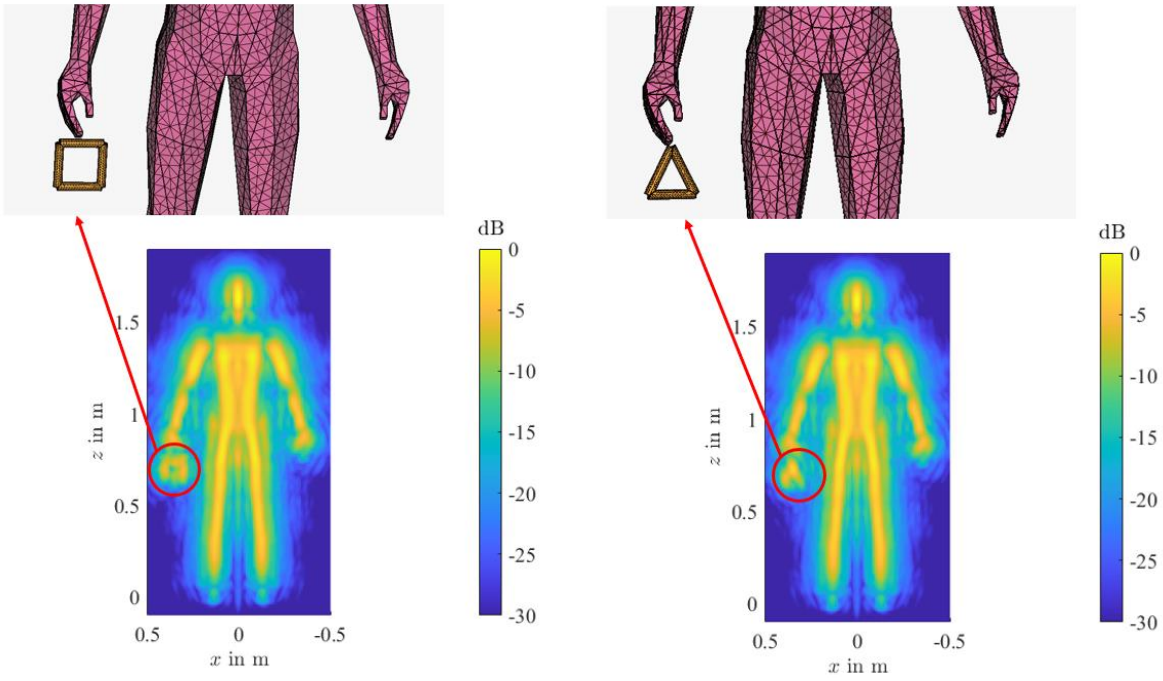

Fig. 9. Imaging results of the human body with different shapes of passive tags. (a) Square-shaped passive tag. (b) Triangular-shaped passive tag.

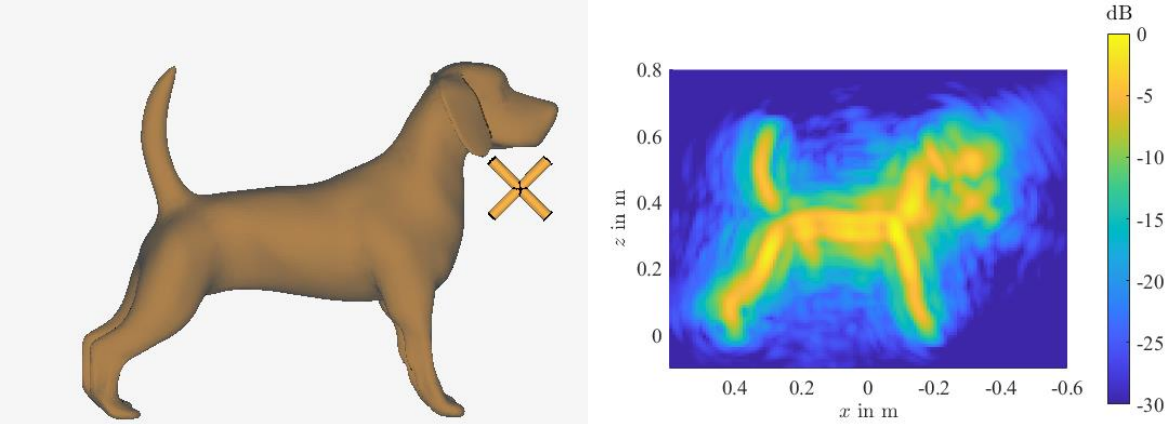

(a) (b)

Fig. 10. (a) Illustration of the simulation setup in FEKO including a dog model and a cross-shaped passive tag. (b) Imaging result.

3.3. Through-the-Wall Imaging

The proposed imaging method and passive tags can also be applied to through-the-wall imaging. As shown in Fig. 11, a concrete wall of sufficient size and 0.1 meters in thickness was placed from $z = -0.1$ m to $z = 0$ m.

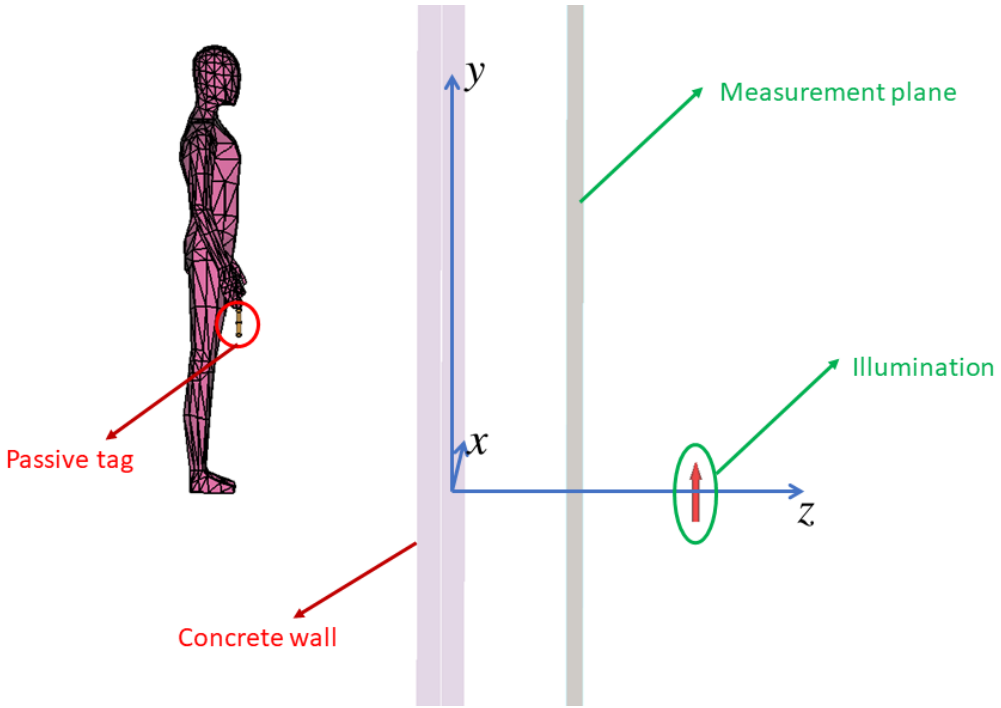

Fig. 11. Illustration of the simulation setup in FEKO, featuring the human body model and the cross-shaped passive tag positioned behind a concrete wall. The illumination source and the NF measurement plane are located on the opposite side of the wall.

The human body model and the cross-shaped passive tag were positioned behind the concrete wall at approximately $z = -1$ m, while a Hertzian dipole serving as the illumination source was placed on the opposite side of the wall at coordinates $x = 0$ m, $y = 0$ m, $z = 1$ m. The x- and y-components of the electric field were collected over a rectangular aperture in the plane $z = 0.5$ m, extending from $x = -3$ m, $y = -3$ m to $x = 3$ m, $y = 3$ m, positioned on the same side of the wall as the dipole. The remaining setup in FEKO remains unchanged. The frequency-dependent relative permittivity $\dot{\varepsilon}_r$ and dielectric loss tangent $\tan\delta$ of the concrete wall, e.g., $\dot{\varepsilon}_r = 2.12$ and $\tan\delta = 0.97$ at 2.02 GHz, are directly loaded from the material library of FEKO. The imaging results in a 2D front view using maximum intensity projection and a 3D point cloud visualization are shown in Fig. 12(a) and Fig. 12(b), respectively. Compared to the cases without the concrete wall, parts of the arms are less visible. However, the main part of the human body and the passive tag are successfully reconstructed with correct phase correction for the through-the-wall propagation path and subsequent coherent superposition. This simulation demonstrates the capability of the proposed method for through-the-wall imaging and localization.

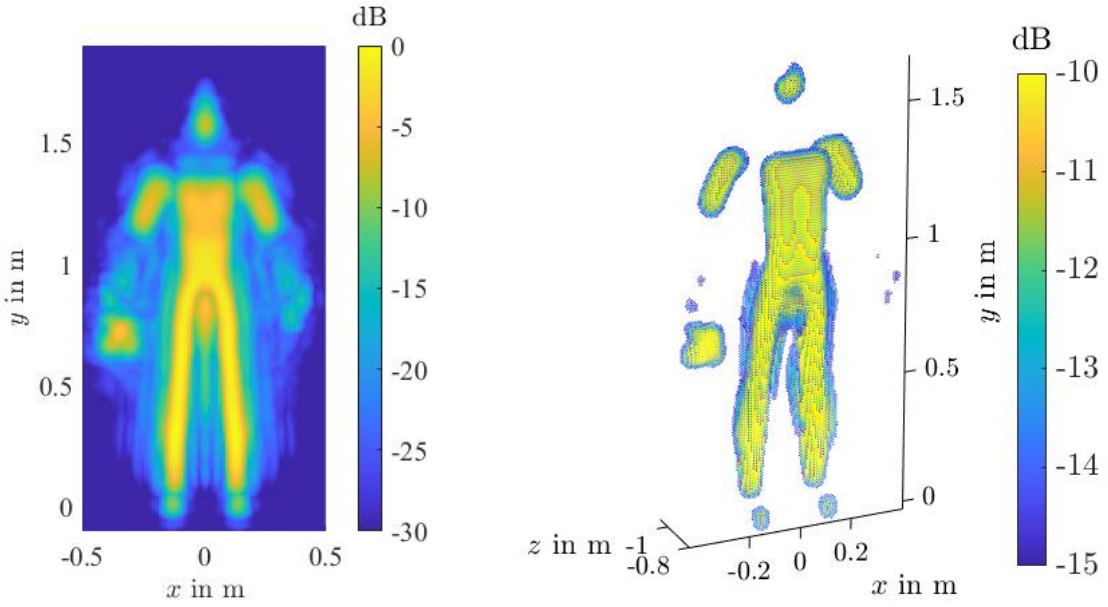

Fig. 12. Imaging results of the human body standing behind the concrete wall with the cross-shaped passive tag. (a) Maximum intensity projection of front view. (b) 3D point cloud visualization.

3.4. Measurement Verification

To further verify the behaviour of the passive tags and the effectiveness of the localization method, several measurement campaigns were conducted in the anechoic antenna measurement chamber at the Technical University of Munich. A mannequin which has been painted with zinc-aluminium spray on the surface, is placed and fixed on the platform, while two double-ridged horn antennas were utilized as the illuminating antenna and the scanning probe as depicted in Fig. 13. The probe

was mounted on a planar scanner, which is capable of mechanically moving along the x- and y-direction in the plane z = 1.8 m. Measurement samples of both co- and cross-polarized field components were taken at 11 110 different positions, uniformly distributed over a rectangular plane extending from x = −1.2 m, y = −1 m to x = 1.2 m, y = 1.2 m. The measurement frequency ranged from 1.5 GHz to 6 GHz with an equal frequency step of 50 MHz. The first measurement was performed without any passive tag. The imaging algorithm was applied for visualization of a target cubic space with the boundaries −0.5 m $\leqslant x \leqslant$ 0.5 m, −1 m $\leqslant y \leqslant$ 1.2 m and -0.1 m $\leqslant z \leqslant$ 0.4 m. The maximum intensity projection for the front view is presented in Fig. 14. Due to the specific scenario setup of passive radar imaging, the image of the mannequin shows stronger induced currents in the region directly facing the illumination source, particularly around the waist. However, the overall shape of the human body has been successfully reconstructed.

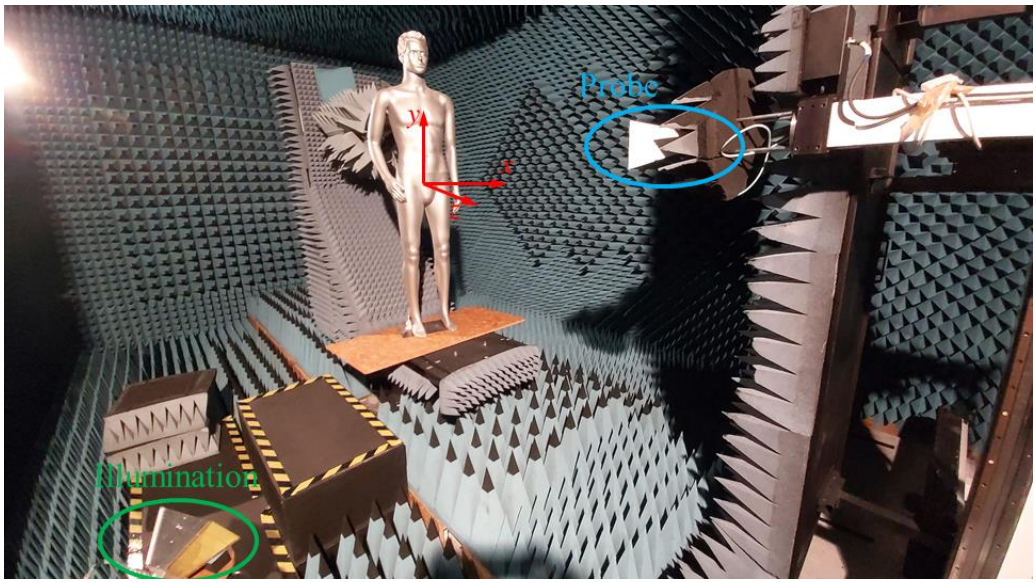

Fig. 13. Measurement configuration utilized in the anechoic chamber. The origin of the coordinate system is set close to the waist of the mannequin.

The second measurement, similar to the previous simulation, involved attaching two patch antennas to the right arm and abdomen of the mannequin using tape, serving as passive tags for indoor positioning, as shown and emphasised by red circles in Fig. 15(a). The patch antennas are narrowband antennas with a resonant frequency of approximately 2.425 GHz, and a close-up image of the antennas is provided in Fig. 15(b). With all measurement parameters kept invariant, the imaging result for this scenario is shown in Fig. 16(a). For comparison, the result without passive tags is provided again in Fig. 16(b). From this comparison, it is evident that two bright spots appear at the locations where the antennas are placed, which can be used as a beacon for determining the precise coordinate of the passive tags. Due to the narrowband radiation characteristic of the antennas, the amplitude of the back-scattered fields are not strong enough across the entire measured frequency band, i.e., the antennas are resonant at around 2.425 GHz while the measurements are performed from 1.5 GHz to 6 GHz. If a wideband antenna that matches the measurement frequency range were used, the imaging performance could be expected to improve.

Nonetheless, when the result in Fig. 16(a) is used as a background and subtracted from Fig. 16(b), the positions of the two antennas become even more pronounced, as shown in Fig. 17.

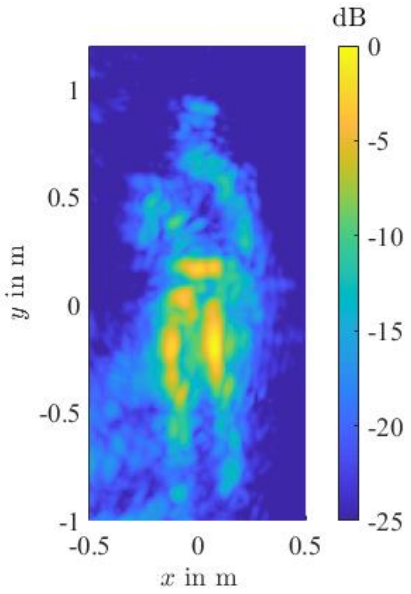

Fig. 14. Imaging result of the mannequin displayed by a maximum intensity projection in front view.

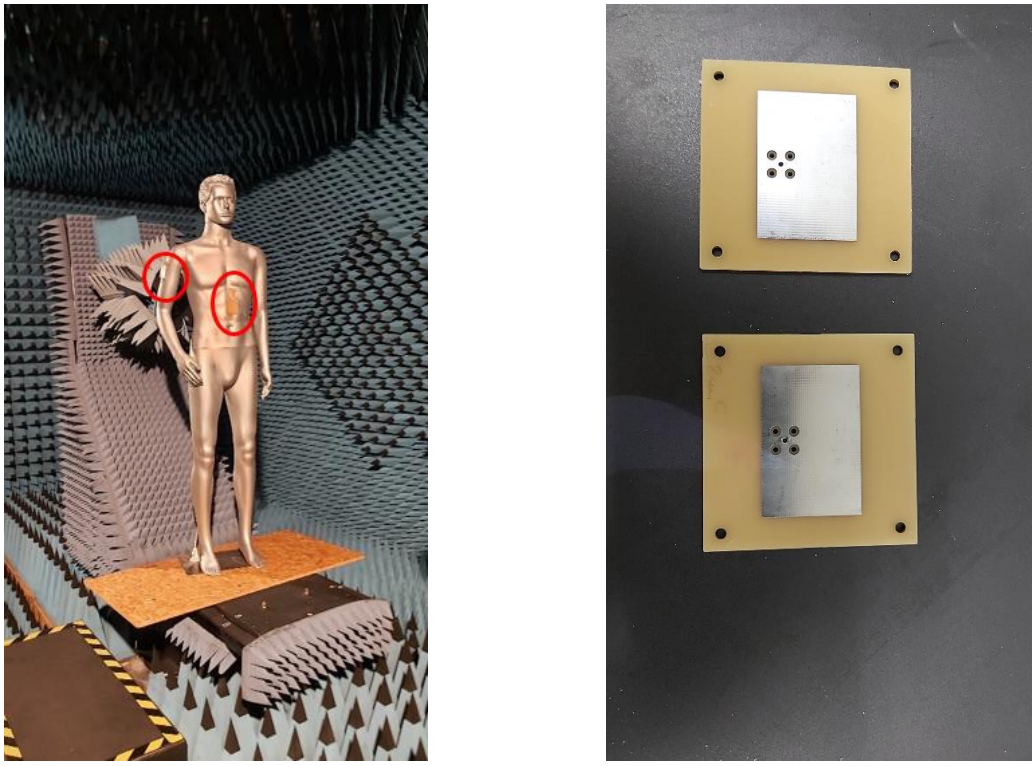

(a) (b)

Fig. 15. (a) Photograph of the mannequin with two passive tags. (b) Close-up image of two patch antennas serving as the passive tags in the measurement.

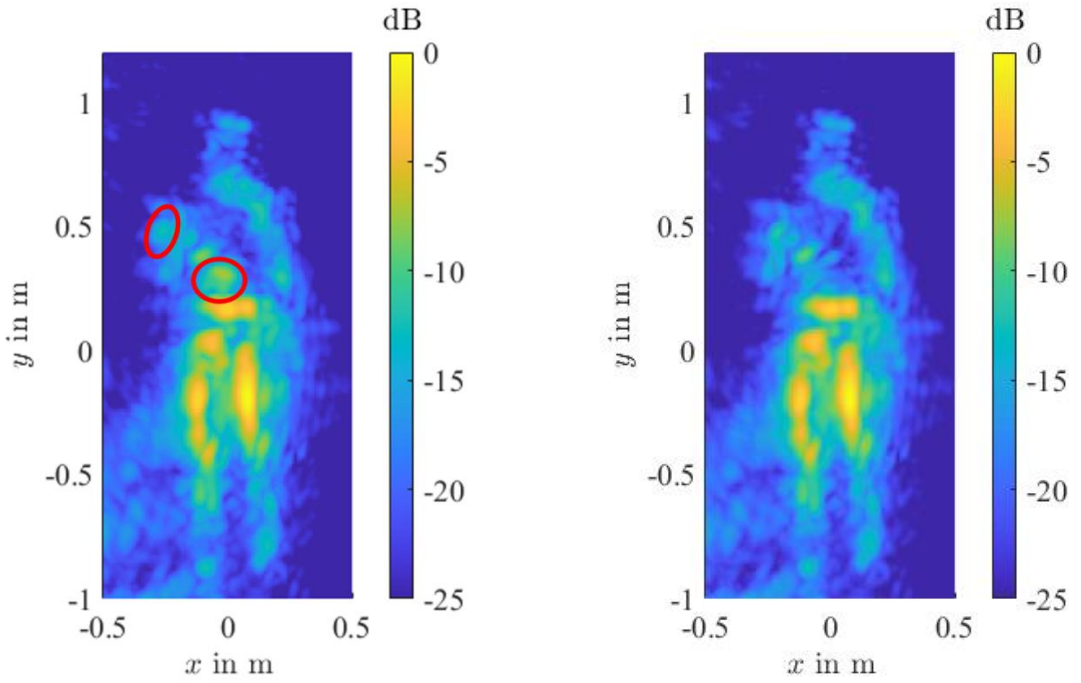

Fig. 16. Imaging results of the mannequin (a) with two passive tags, (b) without passive tags.

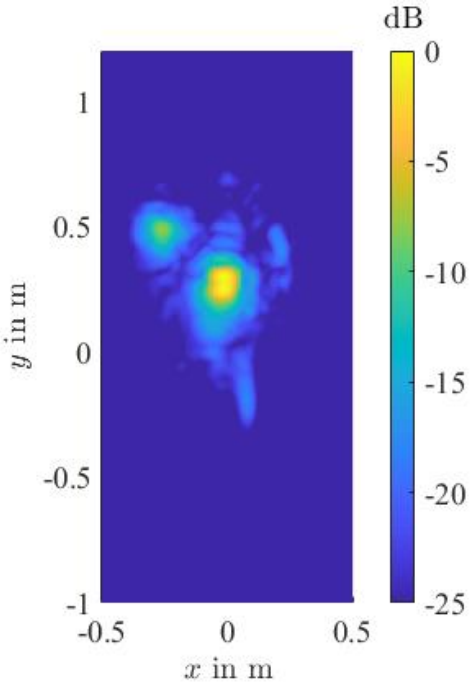

Fig. 17. Imaging result of the passive tags by background subtraction.

3.5. Privacy and Ethical Considerations

As previously mentioned, most current research on indoor localization focuses on developing new technologies and improving accuracy, with little attention paid to privacy and ethical considerations [8]. However, privacy concerns are undeniably critical when localization technology reaches the stage of real-world commercialization. Key challenges include how to effectively achieve precise localization while ensuring user privacy at the fundamental level, how to prevent the leakage of private information while ensuring it is only used for specific purposes, and more importantly, how to establish a mechanism that allows users to trust indoor localization systems and service providers, as pointed out in the ESM [1].

In the context of the HOLDEN project and this deliverable, we aim to grant users full control over the proposed indoor localization technique while achieving high-accuracy localization, thereby fostering privacy trust between users and service providers. Users should be able to customize and control their use of the localization technique. In this deliverable, the privacy and ethical problem are taken in to consideration from the imaging aspect and controllable settings for users, to ensure that this localization technique aligns with privacy and ethical requirements.

3.5.1. Data Collection and Imaging

As mentioned previously in D3.2, at the algorithmic level, our localization method is entirely based on the 3D holographic imaging algorithms outlined in D3.2. During the measurement, by using highly directional antennas or beamforming techniques, users can specify measurements in certain observation domains, thereby restricting the localization algorithm to a particular area.

Additionally, when imaging and localization people or objects within a specific region, the use of differently shaped passive tags, as mentioned earlier, can serve dual purposes, namely identification and as a marker for whether or not the localization algorithms should be applied. Upon detecting a tag of a specific shape, the localization algorithm can, based on pre-defined user rules, filter out specific sources. This allows the algorithm to exclude designated tags from the final localization results, providing users with control over when and where the localization algorithm is applied.

For the imaging aspect, microwave imaging naturally offers stronger privacy protection compared to optical cameras, due to its inherent characteristics. Without further data processing, it is significantly more challenging to extract private information, such as facial features, from microwave imaging results as, e.g., shown in Fig. 16. While future advancements in technologies like machine learning may enable the reconstruction of such features, our algorithm allows users to mitigate this risk by restricting the size of the measurement aperture or limiting the frequency band. This effectively reduces the resolution of the generated images, making such reconstructions more difficult.

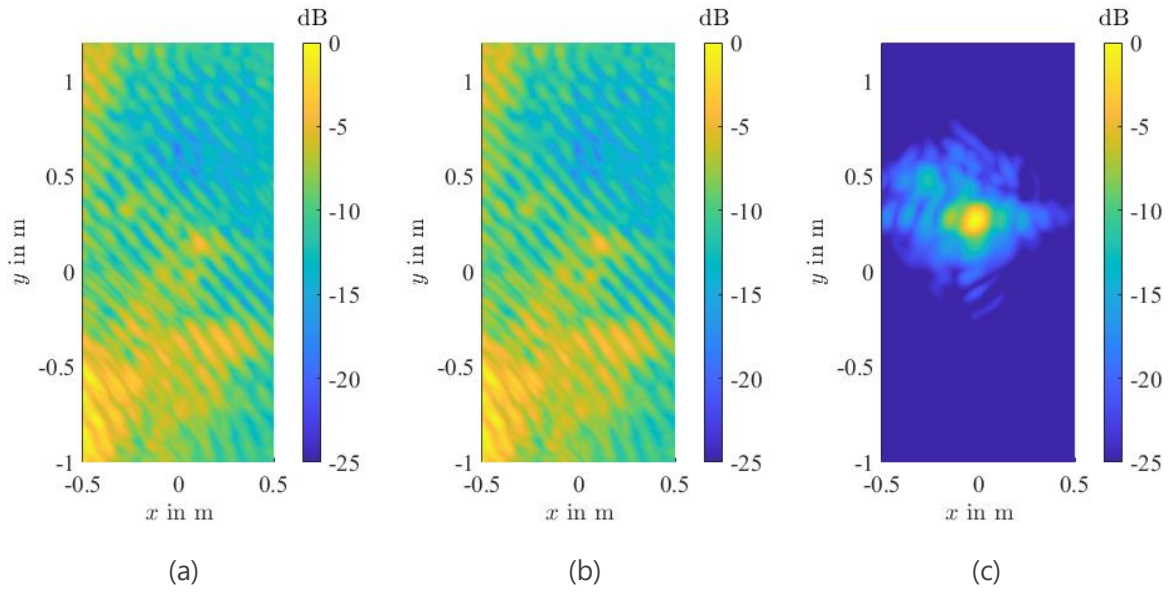

Fig. 18. Imaging result of the mannequin over a frequency range of 2.2 GHz to 2.5 GHz. (a) With passive tags. (b) Without passive tags. (c) After background subtraction.

For instance, in the measurement in Section 3.3, if the frequency is restricted to the range of 2.2 GHz to 2.5 GHz, the imaging results corresponding to Fig. 16(a), Fig. 16(b), and Fig. 17 would appear as depicted in Fig. 18. As can be observed, due to the very limited number of overlapping frequencies, the imaging of the mannequin has almost completely failed. After background subtraction, while the passive tag on the arm of the mannequin is nearly invisible, the tag on the abdomen remains clearly identifiable and can still be accurately reconstructed for positioning purposes. This example demonstrates that with limited bandwidth, the resolution and the imaging performance is reduced and the difficulty in extracting fine details is increased.

3.5.2. Controllable Settings for Users

In addition to privacy considerations at the algorithmic level, we also aim to provide users with full control over customizable settings to enable a tailored positioning algorithm. A straightforward objective in this regard is reducing the intensity of the electromagnetic field scattered by the passive tag. For the simulation scenario shown in Fig. 6, users can simply rotate the tag, such as the case when placing it inside a pocket, as illustrated in Figure 17(a). The cross-shaped passive tag is placed close to the waist of the human body. The corresponding imaging result is shown in Figure 17(b), where it is evident that the passive tag's distinguishability is significantly reduced in this scenario. A similar concept can be applied to the manufacturing of passive tags. By designing the tags to alter their electromagnetic scattering properties, users are granted full control and flexibility in determining how the tags behave. This allows for a customizable approach where the scattering intensity and visibility can be adjusted according to user preferences, thereby enhancing both privacy and control over the positioning system.

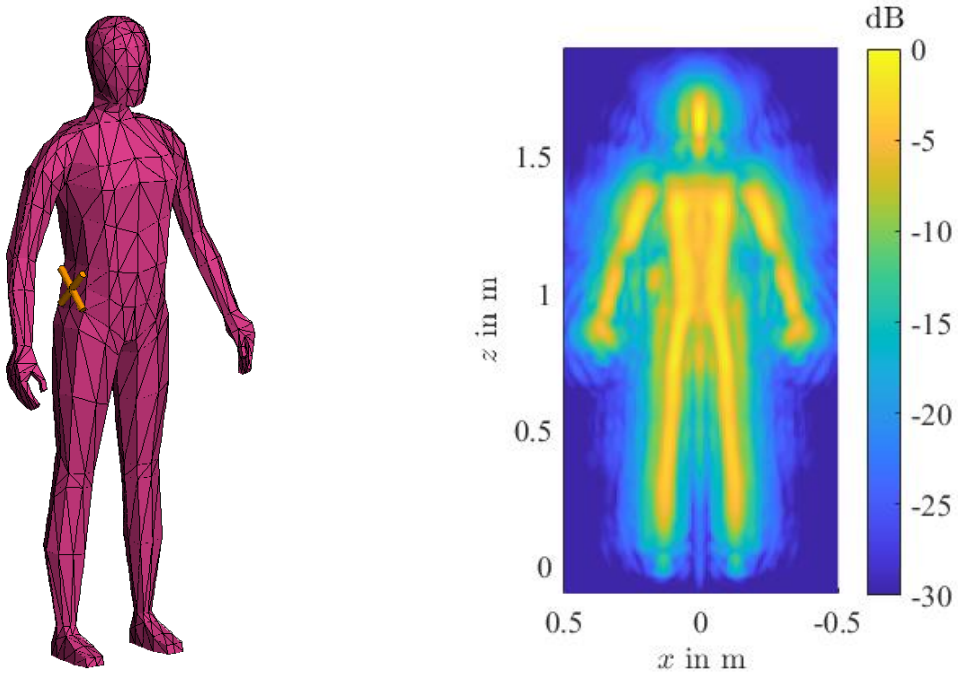

(a) (b)

Fig. 19. (a) Illustration of the simulation setup in FEKO when the cross-shaped passive tag is placed close to the waist of the human body. (b) The corresponding imaging result.

4. Summary

This deliverable discussed an indoor localization system based on 3D holographic imaging technology, as introduced in D3.2. The system utilizes passive tags that rely solely on electromagnetic scattering, eliminating the need for traditional signal transmission or response mechanisms commonly used in other technologies like RFID. The localization method leverages microwave imaging, which inherently offers better privacy protection compared to optical or infrared systems by making it difficult to extract sensitive information, such as facial features, from the imaging results.

The approach allows for the precise localization and identification of people or objects through the use of differently shaped passive tags that can be are detected in the imaging results. Simulations and measurements demonstrate the effectiveness of this technique, even in complex environments, and simulations show how varying the tag design can enable identification, particularly in scenarios where individuals or objects have a similar appearance.

Privacy and ethical considerations are central to this deliverable. One important aspect of ensuring privacy-compliant implementation of this technology is obviously, to allow users the choice of whether or not to wear a passive tag. Additionally, users can manipulate the orientation or placement of passive tags to reduce their visibility in the imaging results. Furthermore, the system incorporates features that allow users to control the measurement parameters, such as limiting the size of the measurement aperture or the frequency band, thereby controlling the resolution of the generated images and protecting user privacy. Another possibility is to automatically detect specific types of passive tags and either retain or remove the corresponding parts in the final image. Thus, privacy issues and ethical concerns can be addressed both at the individual level and by imposing restrictions on the technology itself.

Finally, the deliverable discusses the potential for further customization through the design of passive tags that can alter their electromagnetic scattering characteristics. This gives users more control over their interaction with the system, ensuring that privacy is maintained while allowing for accurate and effective indoor localization.

5. References

[1] S.I. Cammers-Goodwin, N. Gertz, C. Aydin, T. Eibert, M. Nagenborg, S. Savazzi, S. Sigg, "D8.9 ethics status monitor (ESM)", Oct. 2024, Available: https://holden-project.eu/deliverables/

[2] C. Arcadius Tokognon, B. Gao, G. Y. Tian, and Y. Yan, "Structural health monitoring framework based on Internet of Things: A survey," IEEE Internet Things J., vol. 4, no. 3, pp. 619–635, Jun. 2017.

[3] A. Zelenkauskaite, N. Bessis, S. Sotiriadis, and E. Asimakopoulou, "Interconnectedness of complex systems of Internet of Things through social network analysis for disaster management," in 2012 Fourth Int. Conf. Intell. Netw. Collab. Syst., Sep. 2012, pp. 503–508.

[4] D. Snoonian, "Smart buildings," IEEE Spectr., vol. 40, no. 8, pp. 18–23, Aug. 2003.

[5] Zanella, N. Bui, A. Castellani, L. Vangelista, and M. Zorzi, "Internet of Things for smart cities," IEEE Internet Things J., vol. 1, no. 1, pp. 22–32, Feb. 2014.

[6] T. Taleb and A. Kunz, "Machine type communications in 3GPP networks: Potential, challenges, and solutions," IEEE Commun. Mag., vol. 50, no. 3, pp. 178–184, Mar. 2012.

[7] F. Alam, N. Faulkner, and B. Parr, "Device-free localization: A review of non-RF techniques for unobtrusive indoor positioning," IEEE Internet Things J., vol. 8, no. 6, pp. 4228–4249, Mar. 2021.

[8] F. Zafari, A. Gkelias, and K. K. Leung, "A survey of indoor localization systems and technologies," IEEE Commun. Surv. Tutor., vol. 21, no. 3, pp. 2568–2599, 2019.

[9] C. Feng, W. S. A. Au, S. Valaee, and Z. Tan, "Received-signal-strength-based indoor positioning using compressive sensing," IEEE Trans. Mob. Comput., vol. 11, no. 12, pp. 1983–1993, Dec. 2012.

[10] A. S. Paul and E. A. Wan, "RSSI-based indoor localization and tracking using sigma-point Kalman smoothers," IEEE J. Sel. Top. Signal Process., vol. 3, no. 5, pp. 860–873, Oct. 2009.

[11] T.-J. Shan, M. Wax, and T. Kailath, "On spatial smoothing for direction-of-arrival estimation of coherent signals," IEEE Trans. Acoust. Speech Signal Process., vol. 33, no. 4, pp. 806–811, Aug. 1985.

[12] X. Wang, L. Gao, S. Mao, and S. Pandey, "CSI-based fingerprinting for indoor localization: A deep learning approach," IEEE Trans. Veh. Technol., vol. 66, no. 1, pp. 763–776, Jan. 2017.

[13] C. Luo, L. Cheng, M. C. Chan, Y. Gu, J. Li, and Z. Ming, "Pallas: Self-bootstrapping fine-grained passive indoor localization using WiFi monitors," IEEE Trans. Mob. Comput., vol. 16, no. 2, pp. 466–481, Feb. 2017.

[14] J. J. M. Diaz, R. d. A. Mau´es, R. B. Soares, E. F. Nakamura, and C. M. S. Figueiredo, "Bluepass: An indoor Bluetooth-based localization system for mobile applications," in IEEE Symp. Comput. Commun., Jun. 2010, pp. 778–783.

[15] F. J. Gonzalez-Castano and J. García-Reinoso, "Bluetooth location networks," in Proc. IEEE Glob. Telecommun. Conf. (GLOBECOM), vol. 1, 2002, pp. 233–237.

[16] F. Zafari, I. Papapanagiotou, and K. Christidis, "Microlocation for Internet-of-Things-equipped smart buildings," IEEE Internet Things J., vol. 3, no. 1, pp. 96–112, Feb. 2016.

[17] P. Baronti et al., "Wireless sensor networks: A survey on the state of the art and the 802.15.4 and ZigBee standards," Comput. Commun., vol. 30, no. 7, pp. 1655–1695, 2007.

[18] J. Xiong, K. Sundaresan, and K. Jamieson, "ToneTrack: Leveraging frequency-agile radios for time-based indoor wireless localization," in Proc. 21st Annu. Int. Conf. Mobile Comput. Netw., 2015, pp. 537–549.

[19] J. Xu, M. Ma, and C. L. Law, "Position estimation using UWB TDOA measurements," in Proc. IEEE Int. Conf. Ultra-Wideband, 2006, pp. 605–610.

[20] S. Holm, "Hybrid ultrasound-RFID indoor positioning: Combining the best of both worlds," in Proc. IEEE Int. Conf. RFID, Orlando, FL, USA, 2009, pp. 155–162.

[21] L. M. Ni, Y. Liu, Y. C. Lau, and A. P. Patil, "LANDMARC: Indoor location sensing using active RFID," Wireless Netw., vol. 10, no. 6, pp. 701–710, 2004.

[22] A. A. N. Shirehjini, A. Yassine, and S. Shirmohammadi, "An RFIDbased position and orientation measurement system for mobile objects in intelligent environments," IEEE Trans. Instrum. Meas., vol. 61, no. 6, pp. 1664–1675, Jun. 2012.

[23] C. Mariotti, G. Orecchini, M. Virili, F. Alimenti, and L. Roselli, "Wireless localization in buildings by smart tiles," in Proc. IEEE Workshop Environ. Energy Struct. Monitor. Syst. (EESMS), 2012, pp. 7–11.

[24] S. Willis and S. Helal, "A passive RFID information grid for location and proximity sensing for the blind user," vol. 9, Dept. Comput. Inf. Sci. Eng., Univ. Florida, Gainesville, FL, USA, Rep. TR04, 2004.

[25] Y.-S. Kuo, P. Pannuto, K.-J. Hsiao, and P. Dutta, "Luxapose: Indoor positioning with mobile phones and visible light," in Proc. 20th Annu. Int. Conf. Mobile Comput. Netw., 2014, pp. 447–458.

[26] J. Armstrong, Y. A. Sekercioglu, and A. Neild, "Visible light positioning: A roadmap for international standardization," IEEE Commun. Mag., vol. 51, no. 12, pp. 68–73, Dec. 2013.

[27] K. Liu, X. Liu, and X. Li, "Guoguo: Enabling fine-grained indoor localization via smartphone," in Proc. 11th Annu. Int. Conf. Mobile Syst. Appl. Services, 2013, pp. 235–248.

[28] W. Huang et al., "Swadloon: Direction finding and indoor localization using acoustic signal by shaking smartphones," IEEE Trans. Mobile Comput., vol. 14, no. 10, pp. 2145–2157, Oct. 2015.

[29] M. Hazas and A. Hopper, "Broadband ultrasonic location systems for improved indoor positioning," IEEE Trans. Mobile Comput., vol. 5, no. 5, pp. 536–547, May 2006.

[30] N. B. Priyantha, The Cricket Indoor Location System, Ph.D. dissertation, Dept. Elect. Eng. Comput. Sci., Massachusetts Inst. Technol., Cambridge, MA, USA, 2005.

[31] J. Haverinen and A. Kemppainen, "Global indoor self-localization based on the ambient magnetic field", Robot. Auton. Syst., vol. 57, no. 10, pp. 1028-1035, 2009.

[32] T. H. Riehle et al., "Indoor magnetic navigation for the blind", Proc. Annu. Int. Conf. IEEE Eng. Med. Biol. Soc. (EMBC), pp. 1972-1975, 2012.

[33] A. Pedotti, "Simple equipment used in clinical practice for evaluation of locomotion", IEEE Trans. Biomed. Eng., vol. BME-24, no. 5, pp. 456-461, Sep. 1977.

[34] P. Remagnino, G. A. Jones, N. Paragios and C. S. Regazzoni, *Video-Based Surveillance Systems: Computer Vision and Distributed Processing*, Dordrecht, The Netherlands: Kluwer Acad. Publ, 2002.

[35] Y.-L. Hou and G. K. H. Pang, "People counting and human detection in a challenging situation", IEEE Trans. Syst. Man Cybern. A Syst. Humans, vol. 41, no. 1, pp. 24-33, Jan. 2011.

[36] L. Xia, C.-C. Chen and J. K. Aggarwal, "Human detection using depth information by Kinect", Proc. CVPR Workshops, pp. 15-22, 2011.

[37] G. Lu et al., "Where am I in the dark: Exploring active transfer learning on the use of indoor localization based on thermal imaging", Neurocomputing, vol. 173, pp. 83-92, Jan. 2016.

[38] M. M. Rapoport, "The home under surveillance: A tripartite assemblage", Surveillance Soc., vol. 10, no. 3, pp. 320-333, 2012.

[39] N. Ravi, P. Shankar, A. Frankel, A. Elgammal, and L. Iftode, “Indoor localization using camera phones,” in Proc. 7th IEEE Workshop Mob. Comput. Syst. Appl. WMCSA06 Suppl., Aug. 2007, pp. 1–7.

[40] H. Wannous, V. Dovgalecs, R. M´egret, and M. Daoudi, “Place recognition via 3D modeling for personal activity lifelog using wearable camera,” in Int. Conf. Multimed. Model., Klangenfurt, Austria, Jan. 2012, pp. 244– 254.

[41] H. Kawaji, K. Hatada, T. Yamasaki, and K. Aizawa, “Image-based indoor positioning system: Fast image matching using omnidirectional panoramic images,” in Proc. 1st ACM Int. Workshop Multimodal Pervasive Video Anal., New York, NY, USA, Oct. 2010, pp. 1–4.

[42] Body Tissue Dielectric Parameters: https://www.fcc.gov/general/body-tissue-dielectric-parameters, FCC, US. Accessed: 11 Oct. 2023.

[43] Altair. (2024) FEKO. [Online]. Available: https://altairhyperworks.com/product/FEKO

6. Table of Figures